Macromolecules

pubs.acs.org/Macromolecules Article

Ring-Opening Polymerization of Cyclic Esters in an Aqueous Dispersion

Danielle D. Harrier, Paul J. A. Kenis, and Damien Guironnet*

Cite This: *Macromolecules* 2020, 53, 7767−7773 Read Online

ACCESS | Metrics & More | Article Recommendations | Supporting Information

ABSTRACT: Aqueous polymer dispersions are commodity materials produced on a multimillion-ton scale annually. Today none of these materials are biodegradable because the process by which they are made is not compatible with the synthesis of biodegradable polymers. Herein, we report a droplet microfluidic encapsulation strategy for protecting a water incompatible ring-opening polymerization (ROP) catalyst from the aqueous phase, yielding biodegradable polymer particles dispersed in water. Polymerization yields 300 μm sized particles comprised of biodegradable poly(δ-valerolactone) with molecular weights up to 19.5 kg mol^{-1}. The success of this approach relies on simultaneous precise control of the kinetics of polymerization, the rate of mass transfer, and fluid mechanics. The power of this methodology was demonstrated by the synthesis of cross-linked polymer particles through the copolymerization of bis(ε-caprolactone-4-yl)propane and δ-valerolactone, producing cross-linked polymer particles with molecular weights reaching 65.3 kg mol^{-1}. Overall, this encapsulation technique opens the door for the synthesis of biodegradable polymer latex and processable, biodegradable elastomers.

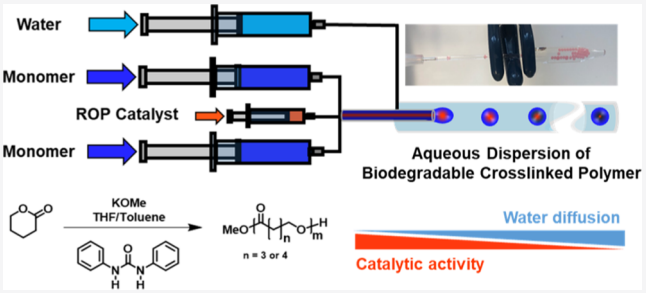

INTRODUCTION

The quest for biodegradable polymers has gained momentum over the past decades, motivated by an alarming accumulation of plastics in landfills and oceans.[1,2] Despite the successful commercialization of many biodegradable thermoplastics targeted at substituting nondegradable polymers, to date no alternative to widely used synthetic and non-biodegradable polymer latexes have been developed.[3−6] A polymer latex is characterized by polymer nanoparticles stabilized by amphiphilic emulsifiers dispersed in an aqueous phase. They account for 10% of the global annual polymer production and are traditionally synthesized through an emulsion polymerization process.[7−9] Polymer latex applications range from coatings,[10,11] adhesives,[12,13] and drug delivery carriers.[14−17] With such a vast range of products, the development of a technique to produce biodegradable polymer latexes would provide a unique opportunity to enhance the sustainability of the polymer industry.

Biodegradable polymers and polymer latexes both possess excellent tunability in fabrication, but they have remained autonomous of one another due to the incompatibility of the polymerization method used to synthesize biodegradable polymers with water.[18,19] Most biodegradable polymers are synthesized through a catalytic ring-opening polymerization (ROP) of aliphatic cyclic esters. The ester bond in the repeating unit makes the polymer susceptible to biological and hydrolytic degradation conferring its biodegradability.[20,21] In industry, the ROP is traditionally performed under moderately anhydrous conditions as water can both deactivate the catalyst and act as an initiator; thus, excess water severely limits the attainable molecular weight.[22−24] In academia, despite the plethora of novel catalysts being developed, most new catalysts are presumed to be quickly and quantitatively deactivated by water and thus are used under purely anhydrous conditions.[25] This water reactivity has thus far categorically prevented the implementation of ROP in an aqueous environment, which would be essential for emulsion polymerization.[26,27]

Miniemulsion polymerization has been successfully implemented for catalytic polymerizations using catalysts that are moderately compatible with water.[28−30] The anionic ROP of high ring strain epoxides has been successfully performed using this technique; however, the high water content limits the molecular weight of the polymer produced ($M_n \leq 730$ g mol^{-1}).[31] In the miniemulsion process, the catalyst and the monomer are combined with a hydrophobic solvent, and the mixture is dispersed into nanodroplets stabilized by a large amount of surfactant using high shear.[32] The polymerization proceeds independently in each droplet to yield the desired

Received: June 2, 2020
Revised: August 20, 2020
Published: September 9, 2020

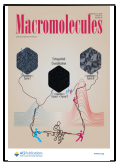

https://dx.doi.org/10.1021/acs.macromol.0c01300
Macromolecules 2020, 53, 7767−7773

nanoparticle dispersion. During the emulsification process, the catalyst/initiator is exposed to both water, which leads to deactivation, and to the monomer, which initiates polymerization.[33] Consequentially, the catalyst needs to be water compatible, and the polymerization needs to remain slow or completely stalled during the emulsification phase.[34,35] For the ROP of cyclic esters, these two requirements have not been met to date, making it incompatible with the miniemulsion process.[25] This limitation, as well as the vast potential for applications of biodegradable polymer latexes, motivated us to develop an alternative encapsulation strategy for performing the ROP in the presence of water.

Our approach consists of utilizing a microfluidic encapsulation strategy where the dispersed phase, comprised of a monomer and a catalyst solution, is fed into a narrow tube to initiate polymerization, before meeting the immiscible continuous aqueous phase at a junction to form micrometer size droplets (Figure 1). The catalyst and monomer solutions

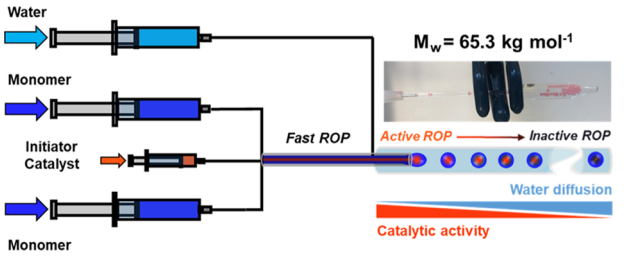

Figure 1. Droplet microfluidic encapsulation of the water-sensitive ring-opening polymerization catalyst. The combination of the fast polymerization and the controlled encapsulation of the catalyst allows the catalyst enough time to polymerize before water diffusion into the droplet can quench the reaction.

are initially supplied from different syringes to prevent premature polymerization before entering the droplet-generating device. The polymerization starts once the catalyst and monomer solutions come in contact and will continue within the droplet until water diffuses throughout the droplet and completely deactivates the catalyst. By design, the catalyst is supplied between the monomer streams to retain the catalyst in the core of the droplets, which is thought to provide more time for the catalyst to remain active before water quenches the polymerization. Water diffusion into the droplet directly limits the polymerization time. Therefore, this approach requires a fast ROP for the polymerization to produce a high-molecular-weight polymer before the water completely deactivates the catalyst.

This report outlines the engineering of a droplet-based microfluidic device that facilitates encapsulation of the water-sensitive catalyst, and allows, for the first time, ROP of synthetic biodegradable linear and partially cross-linked polymers in an aqueous dispersion. Our approach relies on the understanding of fluid mechanics, precise formulation of the polymerization solution, and control over ROP kinetics within the device and the subsequent droplets.

RESULTS AND DISCUSSION

ROP Chemistry Selection. The primary constraint for the success of the encapsulation approach is the selection of a catalyst system that provides a high rate of polymerization, as the time for the polymerization to achieve completion before water diffuses throughout the droplet and deactivates the catalyst is finite. We opted to implement urea organocatalyzed ROP of cyclic esters, because this family of catalysts is known to exhibit fast kinetics and high selectivity (Scheme 1).[36−38]

Scheme 1. Urea Anion Catalysts for the Ring-Opening Polymerization of δ-Valerolactone (VL) and ε-Caprolactone (CL)

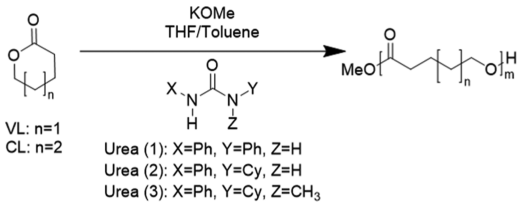

We opted to use δ-valerolactone (VL) and ε-caprolactone (CL) as our monomers for two reasons. First, they yield biodegradable polymers, and second, they are liquid at room temperature, which allows for the preparation of highly concentrated monomer droplets. At concentrations higher than 3 mol L^{-1}, a slight increase of the polymer dispersity and viscosity was observed in batch polymerizations. To avoid pressure build-up or even clogging in the small diameter tubing due to the high viscosity of the neat solution, we chose to operate at a monomer concentration of 3 mol L^{-1} for all subsequent reactions in the flow system. Similarly, the catalyst/initiator solution was made as concentrated as possible; however, the solubility of the initiator, potassium methoxide (KOMe), is highly influenced by the ratio of the catalyst to the initiator. Urea (1) and Urea (2) could be solubilized with a ratio of the initiator:catalyst:monomer of 1:3:200, while Urea (3) needed a 1:4:200 ratio. The high solubility of the catalyst and initiator is preferred to minimize the amount of organic solvent remaining in the final product.

Under this concentration, we confirmed that Urea (1) and Urea (2) exhibit fast rates of polymerizations for VL, with complete conversion in less than 10 s in batch experiments (Figure S1). Urea (2) was identified as a highly active catalyst for CL polymerization and VL/CL copolymerizations.[39,40] We will utilize this reactivity for synthesizing biodegradable elastomeric particles, *vide infra*. Urea (3) suffered from a few disadvantages, including slower polymerization kinetics for both monomers and a lower solubility compared to the other catalysts. Table S1 summarizes the batch polymerization results. Once we identified Urea (1) or Urea (2) as potential catalysts for our system, we proceeded to design the microfluidic device.

Device Design. To perform the ROP in droplets dispersed in water, we implemented a microfluidic device that generates an oil-in-water (O/W) emulsion using a co-flow geometry reactor constructed with commercially available components (Figure 2a).[41−46] By exploiting the unparalleled control over droplet size and encapsulation efficiency intrinsic to droplet-based microfluidics,[47−53] we hypothesized that we could protect the ROP catalyst from water, thus temporarily sustaining catalyst activity in the presence of water.

The organic phase is comprised of two organic streams: the catalyst solution and the monomer solution. The two streams merge in a cross tee and flow through a hypodermic tube, which in turn is being dispersed in water. The choice of the cross tee, with two monomer streams surrounding the catalyst stream, at the inlet is deliberate, as it generates the first level of

https://dx.doi.org/10.1021/acs.macromol.0c01300
Macromolecules 2020, 53, 7767−7773

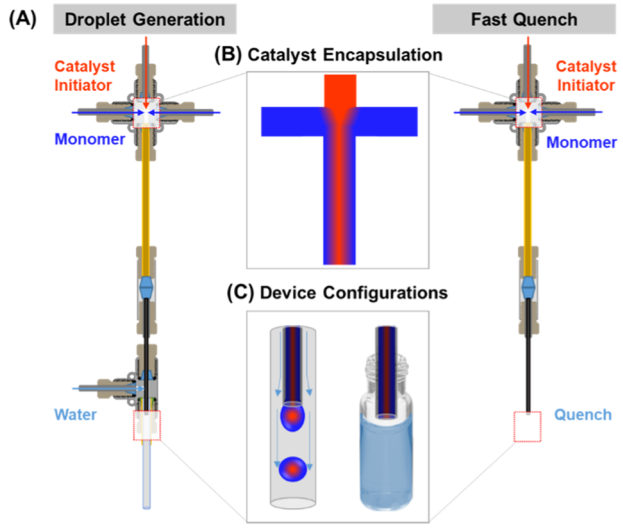

Figure 2. (A) Droplet-generating microfluidic device made from commercially available components. (B) Catalyst encapsulation within two streams of monomer and organic solvent. (C) Droplet (left) and fast quench (right) configurations of the microfluidic device.

protection of the catalytic material. The inherent laminar flow of the fluid in the small diameter, short channel ensures that the catalyst remains primarily in the center of our organic phase since mixing in the tube occurs only via diffusion prior to droplet formation when a sheath flow of water is introduced (Figure 2b).

The diameter of the tubing after the cross tee plays a vital role in the molecular weight and dispersity of the polymer produced.[54−57] Upon reducing the inner diameter of the tubing from 304.8 to 177.8 μm, the diffusion length decreases, which increases the homogeneity of the polymerization solution. In turn, this increase in homogeneity results in an increase in monomer conversion and molecular weight and a decrease in dispersity (Figure S2). Therefore, the final device design utilizes the smallest ID tubing (177.8 μm) after the cross tee to ensure control over the monomer conversion, molecular weight, and dispersity of the polymer generated. Next, we used a standard union tubing connector to attach a short piece of small diameter stainless steel 25G thin wall hypodermic tubing (ID 0.012″ OD 0.02″), which is then fed through the subsequent tee and into the center of a glass capillary. The organic phase expels from the hypodermic tubing in the center of a glass capillary tube, in which the continuous water phase is supplied through a secondary tee and shears the organic phase into droplets. Figure S3 in the Supporting Information provides a more detailed description.

The surface-area-to-volume ratio of the droplet is presumed to impact the polymerization time significantly. A smaller sized droplet has a shorter diffusion path to the core of the particle, which would result in a faster quenching of the catalyst.[58] The organic phase outlet tip (D_{tip}) sets a lower limit for droplet diameter as the tip shields the growing droplet from the shear force of the continuous phase.[59,60] Thus, the droplet diameter could never be smaller than the capillary tip diameter in the dripping flow regime. The 25G hypodermic tubing used here produces approximately 300 μm droplets. This microfluidic design comprised of "off-the-shelf" parts has a fixed reaction volume; thus, the residence time (rt) can only be tuned by varying the flow rate.[61]

To demonstrate that the polymerization proceeds in the aqueous phase after droplet formation, we must precisely determine the monomer conversion at the end of the organic phase outlet tip. Therefore, we ensured that we could operate our device in a second "fast quench" configuration, where the tip of the organic phase outlet is exposed to a quenching solution of acetic acid and tetrahydrofuran (THF) (Figure 2c). After establishing the design of the microfluidic device, we then identified the appropriate formulation and flow rates to achieve excellent control over the size, shape, and homogeneity of the droplets and particles formed.[58]

Droplet Formulation and Flow Rates. Three types of forces influence droplet generation in our system: viscous force, capillary force, and the dominating interfacial force. During droplet generation, the interface deforms significantly due to interfacial tension between the two phases, which results in necking, i.e., the interface fragmenting spontaneously and decaying into disconnected droplets.[62] To determine droplet dynamics, such as fission or droplet break-off, we leveraged the non-dimensionless capillary number (Ca), defined as $Ca = \mu\nu/\gamma$ (where μ is the viscosity of the phase of interest, ν is the velocity of the phase of interest, and γ is the interfacial tension between the two phases) (Figure 3).

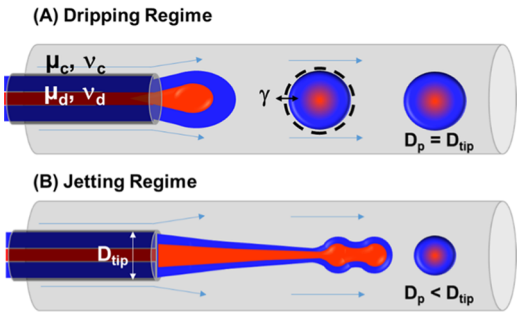

Figure 3. Visual representation of the capillary number parameters and illustration of (A) desired dripping regime and (B) undesirable jetting regime.

Droplet formation requires precise control of each of the parameters in the capillary number, especially the interfacial tension.[63] The interfacial tension of our dispersed phase increases with increasing monomer consumption. At low conversion, the interface between the organic and aqueous phase is miscible, and the surface tension is low, both of which prevent droplet formation. Therefore, we explored hydrophobic solvents that improve the immiscibility of the two phases and expand the range of flow rates for droplet formation. The standard polymerization conditions used to identify a compatible solvent were a 1:3:200 ratio of [initiator]:[catalyst]:[monomer], with a VL monomer concentration of 3 mol L^{-1}. A series of batch polymerizations at room temperature identified toluene as a promising hydrophobic solvent, as it exhibited the fastest rate of living polymerization full conversion within 10 s and produced the highest-molecular-weight polymer (24 kg mol^{-1}) among all solvents tested, Figure S4.

The two other parameters that affect the Ca are velocity and viscosity. Flow velocity is easily controlled in our system by varying the flow rate of both the dispersed and continuous phases. Reliable droplet generation at the organic phase outlet tip with the chosen formulations, the combined flow rate of the two organic phases could not exceed 140 μL/min, which

https://dx.doi.org/10.1021/acs.macromol.0c01300
Macromolecules 2020, 53, 7767−7773

corresponds to a lower limit for the rt of 5 s. The viscosity is a more complicated parameter to control since the viscosity of our dispersed phase is changing as a function of the rt. As the polymerization progresses, the viscosity ratio between our two phases (i.e., $\lambda = \mu_{dispersed}/\mu_{continuous}$) is greater than 1. Also, prior work has shown that the viscous stress of the dispersed phase can impact droplet production since it is difficult for the continuous phase to fragment the dispersed phase.[64,65] This viscous stress makes the dripping-to-jetting transition very sharp, and the only way to remain in the dripping regime is to keep the flow rate ratio of the dispersed to continuous phases (i.e., $Q = Q_{dispersed}/Q_{continuous}$) low, particularly below 0.5 for our device geometry.[66,67] After careful selection of flow rates and formulation, we were able to produce uniform droplets in flow over a broad range of residence times (rt = 5−21 s). We used these flow rates and the formulation to perform the ROP in the microfluidic device.

ROP in Fast Quench Configuration. Before determining how much, if any, polymerization occurred in the dispersed droplet, we precisely determined the conversion at the end of the organic phase outlet tip. To do so, we operated the device in the fast quench configuration, which allowed us to build a rt versus conversion ladder (Figure 4).

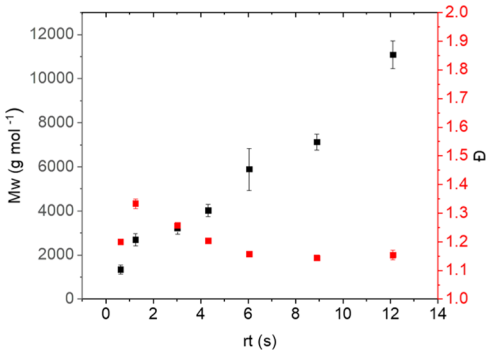

Figure 4. Residence time ladder using the microfluidic device in the fast quench configuration with toluene as the hydrophobic solvent. Reaction conditions: [KOMe]/[urea]/[monomer] = 1:3:200 and $[monomer]_0$ = 3 M in THF at room temperature. M_w and $Đ$ determined by polystrene (PS) calibrated gel permeation chromatography (GPC) in THF.

The molecular weight increases with rt, reaching 10 kg mol^{-1} and a conversion of 50% for a rt of 12 s. The process was stable, as illustrated by the constant conversion achieved for different flow rates over hundreds of residence times (Figure S5). Compared to the batch polymerization, which reaches 100% conversion after 5 s, polymerization in the flow device is significantly slower. Additionally, the molecular weight increases linearly with rt, which differs from batch experiments (Figure S1). Both observations are indicative of the inhomogeneity of the reaction mixture in the tubular reactor. In our flow device, the monomer and catalyst streams are relying exclusively on diffusion to mix. The heterogeneous reaction is diffusion-limited, as the catalyst and initiator THF solution in the center of the organic stream are poorly soluble in the surrounding toluene and monomer. The poor solubility further slows down the homogenization of the solutions and thus the polymerization. While this difference in solubility and slow diffusion impacts polymerization, this difference aids in isolating the catalyst to the center of the droplets, thus delaying quenching by water and restricting the diffusion of the initiator and catalyst into the surrounding water phase.

ROP in Droplet Configuration. Using the same formulation and flow rates as in the fast quench configuration, we performed the ROP in the droplet configuration. By design, we want to keep the monomer conversion low within the microfluidic device to maintain a low enough viscosity of the polymer solution to allow flow through the device without clogging; therefore, we aimed for a rt less than 30 s. While continuing to keep the flow rate ratio less than 0.2, flow rates enabling the formation of the droplets were extremely small. The total dispersed phase flow rate had to stay below 100 μL/min (or a rt greater than 10 s) to obtain consistent droplet formation. At dispersed flow rates greater than 100 μL/min, the dispersed phase shifts into a jetting regime near the hypodermic needle tip before experiencing Rayleigh−Plateau instability and eventually forming droplets downstream (Figure 3b).[63] The molecular weight of the polymer obtained in this jetting regime was similar to the one obtained in the fast quench experiment at identical flow rates (Table 1). We attributed this negative result to the jetting regime exposing more surface area to the aqueous phase before droplet formation, leading to faster quenching of the polymerization.

As mentioned earlier, the flow regime is directly related to the capillary number. The viscosity parameter is dependent on the velocity parameter as the flow rate of the solution, in conjunction with the polymerization rate, determines the viscosity of the solution. Therefore, we focused our attention on the difference in interfacial tension between the two streams. We hypothesized that we could extend the flow rates that produced the desired dripping regime by adding a surfactant in the aqueous phase. Indeed, in the presence of 1% of Tergitol in the aqueous phase, the droplet break-off at the hypodermic needle tip was sharp and consistent across a broad

Table 1. Comparison of Droplet Reactor Polymerization Performance[a]

entry	configuration	water	time (s)	X (%)[b]	$M_{n,\,theor}$ (g mol^{-1})	M_w[c] (g mol^{-1})	$Đ$[c]
1	batch		10	90	18 000	20 700	1.2
2	batch	+100 equiv	120	0	0	0	
3	fast quench	no	10	26	5200	7700	1.3
4	droplet jetting to the dripping regime	yes	10	27	5400	7900	1.3
5[d]	droplet dripping regime with the surfactant	yes	10	55	11 000	13 800	1.6
6[e]	droplet dripping regime with the cross-linker	yes	10	N/A	N/A	45 200	2.4

[a]Reaction conditions: [KOMe]/[urea]/[monomer] = 1:3:200 and $[monomer]_0$ = 3 M in THF at room temperature. All batch reactions performed under anhydrous conditions and quenched with benzoic acid. [b]Conversion determined by ^{1}H NMR. [c]M_w and dispersity $Đ$ determined by PS calibrated GPC in THF. [d]Tergitol 1% added to the continuous water phase. [e]2,2-Bis(ε-caprolactone-4-yl)propane (BCP) cross-linker 0.5% added to the monomer streams.

https://dx.doi.org/10.1021/acs.macromol.0c01300
Macromolecules 2020, 53, 7767−7773

set of residence time (5−21 s) (Video S1). In the presence of a surfactant, the polymer formed in the droplet reached a molecular weight and conversion double that of the fast quench setup. The clear difference in the molecular weight of the polymer formed between the droplet regime and the fast quench demonstrates that polymerization proceeds in the droplet (Table 1, entry 5).

Interestingly, the dispersity of the polymer obtained in the droplet configuration is broader than in any other setup with an asymmetrical distribution skewed toward lower molecular weight (Figure S6). This asymmetrical distribution is consistent with the absence of chain transfer and the slow quenching of the polymerization caused by the diffusion of water, further validating that the polymerization proceeded in the droplet. We confirmed this result by performing a systematic study where the molecular weight of the polymer synthesized at several residence times was compared between the fast quench and droplet configuration. At each tested rt, the droplet encapsulation technique produced higher-molecular-weight polymers compared to fast quench (Figure 5). This higher molecular weight demonstrates, for the first time, successful ring-opening polymerization of biodegradable cyclic esters in an aqueous dispersion.

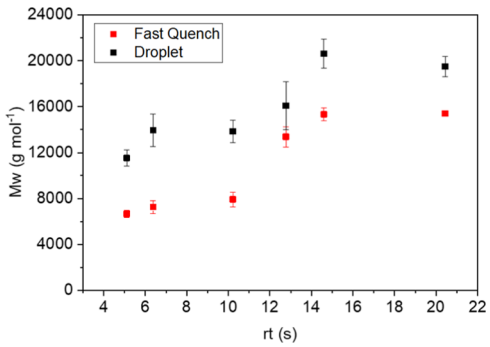

Figure 5. Comparison between the molecular weight of the polymer produced using the fast quench and droplet generation configuration Reaction conditions: [KOMe]/[urea]/[monomer] = 1:3:200 and $[monomer]_0$ = 3 M in THF at room temperature. Mw determined by PS calibrated GPC in THF. Fast quench configuration: quenching solution is acetic acid. Droplet generation configuration: Tergitol 1% added to the continuous water phase.

To demonstrate the benefit of performing a ROP in dispersion, we aimed to synthesize biodegradable elastomer particles by introducing a cross-linking monomer within the dispersed phase. We chose 2,2-bis(ε-caprolactone-4-yl)-propane (BCP), because this cross-linker is compatible with the urea organocatalyzed ROP (Scheme 2).[68,69] We maintained the polymerization conditions used above, but the catalyst was switched from Urea 1 to Urea 2 to allow for the copolymerization of the VL monomer with the CL-based cross-linker. Slight modifications to the device were made to prevent increased pressure and potential clogging from the higher viscosity of the cross-linked polymer solution, refer to Figure S8 for more details. The addition of a 0.5% loading of BCP led to a dramatic increase in molecular weight to 45.2 kg mol^{-1} in 10 s (Table 1 entry 6). The dispersity of the resulting polymer simultaneously increased to 2.4, consistent with the presence of cross-linking.

When comparing the fast quench to droplet configuration for a range of rt between 5 and 13 s, the polymer obtained from the droplet polymerizations showed higher molecular weight for every flow rate tested (Figure S10). After increasing the loading of the BCP to 1%, we produced cross-linked particles with a molecular weight of 65.3 kg mol^{-1} and a dispersity of 2.6 (Figure S9). The cross-linked polymer droplets still contained the hydrophobic solvent, toluene, and therefore were not robust solid particles. After the device formed the droplets, methanol was added to the aqueous colloidal dispersion in the collection vessel allowing the excess toluene and residual reaction material to diffuse out of the droplets. This extraction of solvent and the residual monomer yielded solid particles (Video S2). Through the introduction of the cross-linker BCP, we were able to expand the use of the encapsulation technique to produce cross-linked biodegradable materials in flow.

Scheme 2. Urea Anion Catalysts for the Ring-Opening Polymerization of δ-Valerolactone and Cross-linking With 2,2-Bis(ε-caprolactone-4-yl)propane (BCP)

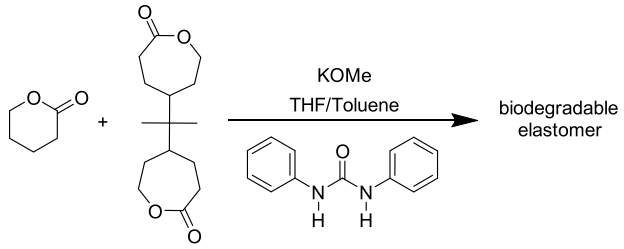

CONCLUSIONS

With the development of this encapsulation technique for water-sensitive ring-opening polymerization catalysts, we have demonstrated, for the first time, ROP in an aqueous dispersion, as well as the generation of cross-linked biodegradable elastomer droplets in flow. Through device design and understanding of fluid mechanics, we were able to encapsulate the water-sensitive urea organocatalysts in between monomer and hydrophobic solvent. The heterogeneous polymerization protected the urea catalyst from the aqueous phase, allowing polymerization to proceed while in the aqueous phase. The droplet ROP encapsulation was able to produce a maximum molecular weight of 20.6 kg mol^{-1} compared to the fast quench configuration maximum of 15.3 kg mol^{-1}. This encapsulation technique offers a wide variety of tunability of the polymer particles produced. To illustrate this, we introduced a cross-linking monomer into the formulation to produce biodegradable elastomer particles. The molecular weight of the resulting elastomer droplets reached a maximum of 65.3 kg mol^{-1} with a dispersity of 2.6, confirming that cross-linking had occurred. These particles can then be isolated and processed similarly to non-biodegradable coagulated latex, e.g., styrene butadiene rubber and natural rubber, offering a sustainable alternative to the accumulation of a non-biodegradable thermoset-based object in our landfills. Further work into the functionalization of these particles for more advanced applications could further a diverse field of research, including coatings, drug delivery, and biomedical applications.

ASSOCIATED CONTENT

Supporting Information

The Supporting Information is available free of charge at https://pubs.acs.org/doi/10.1021/acs.macromol.0c01300.

https://dx.doi.org/10.1021/acs.macromol.0c01300
Macromolecules 2020, 53, 7767−7773

Droplet break-off at the hypodermic needle tip was sharp and consistent across a broad set of residence time (5−21 s) (Video S1) (MP4)

Extraction of solvent and the residual monomer yielded solid particles (Video S2) (MP4)

Results from testing three urea organocatalyst with hydrophobic solvent (Table S1); results from batch experiments comparing the three catalysts rate of polymerization of VL (Figure S1); hows the effect of the diameter of the tubing after the cross tee on the molecular weight, polydispersity, and conversion of the polymer produced (Figure S2); droplet generating co-flow microfluidic device with all components listed (Figure S3) (PDF)

AUTHOR INFORMATION

Corresponding Author

Damien Guironnet − *Department of Chemical and Biomolecular Engineering, University of Illinois, Urbana—Champaign, Urbana, Illinois 61801, United States;* orcid.org/0000-0002-0356-6697; Email: guironne@illinois.edu

Authors

Danielle D. Harrier − *Department of Chemical and Biomolecular Engineering, University of Illinois, Urbana—Champaign, Urbana, Illinois 61801, United States*

Paul J. A. Kenis − *Department of Chemical and Biomolecular Engineering, University of Illinois, Urbana—Champaign, Urbana, Illinois 61801, United States;* orcid.org/0000-0001-7348-0381

Complete contact information is available at: https://pubs.acs.org/10.1021/acs.macromol.0c01300

Author Contributions

Device design, fabrication, and experiments were performed by D.D.H. The manuscript was written through the contributions of all authors. All authors have given approval to the final version of the manuscript.

Notes

The authors declare no competing financial interest.

ACKNOWLEDGMENTS

This material is based upon work supported by the National Science Foundation Graduate Research Fellowship under Grant No. DGE- 1746047 and the National Science Foundation through Grant CBET 17-06911. The authors would like to thank Kavisha Baxi for her help with the batch experiments.

ABBREVIATIONS

ROP ring-opening polymerization; rt residence time; VL δ-valerolactone; CL ε-caprolactone; BCP bis(ε-caprolactone-4-yl)propane; Ca capillary number; PS polystyrene

REFERENCES

(1) Vasanthi, K. Biodegradable Polymers—A Review. *Polym. Sci.* **2017**, *3*, 1−7.

(2) Gilbert, M. Plastics Materials. In *Brydson's Plastics Materials*; Elsevier, 2017; pp 1−18.

(3) Geyer, R.; Jambeck, J. R.; Law, K. L. Production, Use, and Fate of All Plastics Ever Made. *Sci. Adv.* **2017**, *3*, e1700782.

(4) Song, R.; Murphy, M.; Li, C.; Ting, K.; Soo, C.; Zheng, Z. Current Development of Biodegradable Polymeric Materials for Biomedical Applications. *Drug Des., Dev. Ther.* **2018**, *12*, 3117−3145.

(5) Armentano, I.; Dottori, M.; Fortunati, E.; Mattioli, S.; Kenny, J. M. Biodegradable Polymer Matrix Nanocomposites for Tissue Engineering: A Review. *Polym. Degrad. Stab.* **2010**, *95*, 2126−2146.

(6) Webb, H. K.; Arnott, J.; Crawford, R. J.; Ivanova, E. P. Plastic Degradation and Its Environmental Implications with Special Reference to Poly(Ethylene Terephthalate). *Polymers* **2013**, *5*, 1−18.

(7) Nomura, M.; Tobita, H.; Suzuki, K. Emulsion Polymerization: Kinetic and Mechanistic Aspects. *Adv. Polym. Sci.* **2005**, *175*, 1−128.

(8) Chern, C. S. Emulsion Polymerization Mechanisms and Kinetics. *Prog. Polym. Sci.* **2006**, *31*, 443−486.

(9) Chern, C.-S. *Principles and Applications of Emulsion Polymerization*; John Wiley & Sons, Inc.: Hoboken, NJ, 2008.

(10) Deniau, G.; Azoulay, L.; Bougerolles, L.; Palacin, S. Surface Electroinitiated Emulsion Polymerization: Grafted Organic Coatings from Aqueous Solutions. *Chem. Mater.* **2006**, *18*, 5421−5428.

(11) Tsavalas, J. G.; Sundberg, D. C. Hydroplasticization of Polymers: Model Predictions and Application to Emulsion Polymers. *Langmuir* **2010**, *26*, 6960−6966.

(12) Sakdapipanich, J.; Thananusont, N.; Pukkate, N. Synthesis of Acrylate Polymers by a Novel Emulsion Polymerization for Adhesive Applications. *J. Appl. Polym. Sci.* **2006**, *100*, 413−421.

(13) Khromiak, U.; Levytskyi, V.; Stepova, K.; Tarnawsky, A. Synthesis and Properties of Adhesive Polymer-Methylmethacrylate Materials. *Int. J. Polym. Sci.* **2018**, *2018*, 1−9.

(14) Reverchon, E.; Adami, R.; Cardea, S.; Porta, G. Della. Supercritical Fluids Processing of Polymers for Pharmaceutical and Medical Applications. *J. Supercrit. Fluids* **2009**, 484−492.

(15) Colombo, C.; Morosi, L.; Bello, E.; Ferrari, R.; Licandro, S. A.; Lupi, M.; Ubezio, P.; Morbidelli, M.; Zucchetti, M.; DIncalci, M.; Moscatelli, D.; Frapolli, R. PEGylated Nanoparticles Obtained through Emulsion Polymerization as Paclitaxel Carriers. *Mol. Pharmaceutics* **2016**, *13*, 40−46.

(16) Soppimath, K. S.; Aminabhavi, T. M.; Kulkarni, A. R.; Rudzinski, W. E. Biodegradable Polymeric Nanoparticles as Drug Delivery Devices. *J. Controlled Release* **2001**, *70*, 1−20.

(17) Freiberg, S.; Zhu, X. X. Polymer Microspheres for Controlled Drug Release. *Int. J. Pharm.* **2004**, 1−18.

(18) Gross, R. A.; Kalra, B. Biodegradable Polymers for the Environment. *Science* **2002**, *297*, 803−807.

(19) Madhavan Nampoothiri, K.; Nair, N. R.; John, R. P. An Overview of the Recent Developments in Polylactide (PLA) Research. *Bioresour. Technol.* **2010**, *101*, 8493−8501.

(20) Okada, M. Chemical Syntheses of Biodegradable Polymers. *Prog. Polym. Sci.* **2002**, *27*, 87−133.

(21) Hopewell, J.; Dvorak, R.; Kosior, E. Plastics Recycling: Challenges and Opportunities. *Philos. Trans. R. Soc., B* **2009**, *364*, 2115−2126.

(22) Amass, W.; Amass, A.; Tighe, B. A Review of Biodegradable Polymers: Uses, Current Developments in the Synthesis and Characterization of Biodegradable Polyesters, Blends of Biodegradable Polymers and Recent Advances in Biodegradation Studies. *Polym. Int.* **1998**, *47*, 89−144.

(23) Tiwari, A.; Titinchi, S. *Advanced Catalytic Materials*; John Wiley & Sons, Inc.: Hoboken, NJ, 2015.

(24) Siparsky, G. L.; Voorhees, K. J.; Miao, F. Hydrolysis of Polylactic Acid (PLA) and Polycaprolactone (PCL) in Aqueous Acetonitrile Solutions: Autocatalysis. *J. Polym. Environ.* **1998**, *6*, 31−41.

(25) Walsh, D. J.; Hyatt, M. G.; Miller, S. A.; Guironnet, D. Recent Trends in Catalytic Polymerizations. *ACS Catal.* **2019**, *9*, 11153−11188.

(26) Hungenberg, K.-D.; Jahns, E. Trends in Emulsion Polymerization Processes from an Industrial Perspective. *Adv. Polym. Sci.* **2017**, *280*, 195−214.

(27) Zhao, H.; Nathaniel, G. A.; Merenini, P. C. Enzymatic Ring-Opening Polymerization (ROP) of Lactides and Lactone in Ionic

Liquids and Organic Solvents: Digging the Controlling Factors. *RSC Adv.* **2017**, *7*, 48639−48648.
(28) Mecking, S.; Held, A.; Bauers, F. M. Aqueous Catalytic Polymerization of Olefins. *Angew. Chem., Int. Ed.* **2002**, *41*, 544−561.
(29) Mecking, S. State-of-the-Art. In *Multiphase Homogeneous Catalysis*; Wiley-VCH Verlag GmbH: Weinheim, Germany, 2008; pp 763−764.
(30) Mecking, S. Polymer Dispersions from Catalytic Polymerization in Aqueous Systems. *Colloid Polym. Sci.*. **2007**, 605−619.
(31) Maitre, C.; Ganachaud, F.; Ferreira, O.; Lutz, J. F.; Paintoux, Y.; Hémery, P. Anionic Polymerization of Phenyl Glycidyl Ether in Miniemulsion. *Macromolecules* **2000**, *33*, 7730−7736.
(32) Teixeira, R. F. A.; Bon, S. A. F. *Hybrid Latex Particles*; van Herk, A. M.; Landfester, K., Eds.; Springer: Berlin, Heidelberg, 2010; Vol. *233*.
(33) van Herk, A. M. *Chemistry and Technology of Emulsion Polymerisation*; van Herk, A. M., Ed.; John Wiley & Sons Ltd: Oxford, U.K., 2013.
(34) DeKock, R. L.; Hristov, J. H.; Anderson, G. D. W.; Göttker-Schnetmann, I.; Mecking, S.; Ziegler, T. Possible Side Reactions Due to Water in Emulsion Polymerization by Late Transition Metal Complexes II: Deactivation of the Catalyst by a Wacker-Type Reaction. *Organometallics* **2005**, *24*, 2679−2687.
(35) Daniels, E. S.; Sudol, E. D.; El-Aasser, M. S. *Polymer Colloids*; ACS Symposium Series; American Chemical Society: Washington, DC, 2001; Vol. *801*.
(36) Kamber, N. E.; Jeong, W.; Waymouth, R. M.; Pratt, R. C.; Lohmeijer, B. G. G.; Hedrick, J. L. Organocatalytic Ring-Opening Polymerization. *Chem. Rev.* **2007**, *107*, 5813−5840.
(37) Dove, A. P. Organic Catalysis for Ring-Opening Polymerization. *ACS Macro Lett.* **2012**, 1409−1412.
(38) Lin, B.; Hedrick, J. L.; Park, N. H.; Waymouth, R. M. Programmable High-Throughput Platform for the Rapid and Scalable Synthesis of Polyester and Polycarbonate Libraries. *J. Am. Chem. Soc.* **2019**, *141*, 8921−8927.
(39) Lin, B.; Waymouth, R. M. Organic Ring-Opening Polymerization Catalysts: Reactivity Control by Balancing Acidity. *Macromolecules* **2018**, *51*, 2932−2938.
(40) Lin, B.; Waymouth, R. M. Urea Anions: Simple, Fast, and Selective Catalysts for Ring-Opening Polymerizations. *J. Am. Chem. Soc.* **2017**, *139*, 1645−1652.
(41) Christopher, G. F.; Anna, S. L. Microfluidic Methods for Generating Continuous Droplet Streams. *J. Phys. D: Appl. Phys.* **2007**, *40*, 319−336.
(42) Janiesch, J. W.; Weiss, M.; Kannenberg, G.; Hannabuss, J.; Surrey, T.; Platzman, I.; Spatz, J. P. Key Factors for Stable Retention of Fluorophores and Labeled Biomolecules in Droplet-Based Microfluidics. *Anal. Chem.* **2015**, *87*, 2063−2067.
(43) Liu, K.; Lepin, E. J.; Wang, M. W.; Guo, F.; Lin, W. Y.; Chen, Y. C.; Sirk, S. J.; Olma, S.; Phelps, M. E.; Zhao, X. Z.; Tseng, H. R.; Van Dam, R. M.; Wu, A. M.; Shen, C. K. F. Microfluidic-Based 18F-Labeling of Biomolecules for Immuno-Positron Emission Tomography. *Mol. Imaging* **2011**, *10*, 168−176.
(44) Hans, M.; Lowman, A. Biodegradable Nanoparticles for Drug Delivery and Targeting. *Curr. Opin. Solid State Mater. Sci.* **2002**, *6*, 319−327.
(45) Hu, X.; Zhu, N.; Fang, Z.; Guo, K. Continuous Flow Ring-Opening Polymerizations. *React. Chem. Eng.* **2017**, 20−26.
(46) Reis, M. H.; Leibfarth, F. A.; Pitet, L. M. Polymerizations in Continuous Flow: Recent Advances in the Synthesis of Diverse Polymeric Materials. *ACS Macro Lett.* **2020**, *9*, 123−133.
(47) Zhu, P.; Wang, L. Passive and Active Droplet Generation with Microfluidics: A Review. *Lab Chip* **2017**, *17*, 34−75.
(48) Stutman, D. R.; Klein, A.; El-Aasser, M. S.; Vanderhoff, J. W. Mechanism of Core/Shell Emulsion Polymerization. *Ind. Eng. Chem. Prod. Res. Dev.* **1985**, *24*, 404−412.
(49) Shah, R. K.; Shum, H. C.; Rowat, A. C.; Lee, D.; Agresti, J. J.; Utada, A. S.; Chu, L. Y.; Kim, J. W.; Fernandez-Nieves, A.; Martinez, C. J.; Weitz, D. A. Designer Emulsions Using Microfluidics. *Mater. Today* **2008**, 18−27.
(50) Bottaro, E.; Nastruzzi, C. "Off-the-Shelf" Microfluidic Devices for the Production of Liposomes for Drug Delivery. *Mater. Sci. Eng., C* **2016**, *64*, 29−33.
(51) Gu, F.; Farokhzad, O. C.; Kyei-Manu, W.; Cannizzaro, C.; Karnik, R.; Dean, L.; Basto, P.; Langer, R. Microfluidic Platform for Controlled Synthesis of Polymeric Nanoparticles. *Nano Lett.* **2008**, *8*, 2906−2912.
(52) Dorresteijn, R.; Haschick, R.; Klapper, M.; Müllen, K. Poly(L-Lactide) Nanoparticles via Ring-Opening Polymerization in Non-Aqueous Emulsion. *Macromol. Chem. Phys.* **2012**, *213*, 1996−2002.
(53) Mei, L.; Jin, M.; Xie, S.; Yan, Z.; Wang, X.; Zhou, G.; Van Den Berg, A.; Shui, L. A Simple Capillary-Based Open Microfluidic Device for Size on-Demand High-Throughput Droplet/Bubble/Microcapsule Generation. *Lab Chip* **2018**, *18*, 2806−2815.
(54) Hessel, V.; Renken, A.; Schouten, J. C.; Yoshida, J. I. *Micro Process Engineering: A Comprehensive Handbook*; Hessel, V.; Renken, A.; Schouten, J. C.; Yoshida, J.-I., Eds.; Wiley-VCH: Weinheim, Germany, 2013; Vol. *1*.
(55) Eckardt, O.; Wenn, B.; Biehl, P.; Junkers, T.; Schacher, F. H. Facile Photo-Flow Synthesis of Branched Poly(Butyl Acrylate)S. *React. Chem. Eng.* **2017**, *2*, 479−486.
(56) Reis, M. H.; Varner, T. P.; Leibfarth, F. A. The Influence of Residence Time Distribution on Continuous-Flow Polymerization. *Macromolecules* **2019**, *52*, 3551−3557.
(57) Corrigan, N.; Zhernakov, L.; Hashim, M. H.; Xu, J.; Boyer, C. Flow Mediated Metal-Free PET-RAFT Polymerisation for Upscaled and Consistent Polymer Production. *React. Chem. Eng.* **2019**, *4*, 1216−1228.
(58) Teh, S. Y.; Lin, R.; Hung, L. H.; Lee, A. P. Droplet Microfluidics. *Lab Chip* **2008**, 198−220.
(59) Erb, R. M.; Obrist, D.; Chen, P. W.; Studer, J.; Studart, A. R. Predicting Sizes of Droplets Made by Microfluidic Flow-Induced Dripping. *Soft Matter* **2011**, *7*, 8757−8761.
(60) Deng, C.; Huang, W.; Wang, H.; Cheng, S.; He, X.; Xu, B. Preparation of Micron-Sized Droplets and Their Hydrodynamic Behavior in Quiescent Water. *Braz. J. Chem. Eng.* **2018**, *35*, 709−720.
(61) Wang, Y.; Wu, P.; Luo, Z.; Li, Y.; Liao, M.; Li, Y.; He, L. Controllable Geometry-Mediated Droplet Fission Using "off-the-Shelf" Capillary Microfluidics Device. *RSC Adv.* **2014**, *4*, 31184−31187.
(62) Seemann, R.; Brinkmann, M.; Pfohl, T.; Herminghaus, S. Droplet Based Microfluidics. *Rep. Prog. Phys.* **2012**, *75*, 016601.
(63) Nunes, J. K.; Tsai, S. S. H.; Wan, J.; Stone, H. A. Dripping and Jetting in Microfluidic Multiphase Flows Applied to Particle and Fibre Synthesis. *J. Phys. D: Appl. Phys.* **2013**, *46*, 114002.
(64) Nekouei, M.; Vanapalli, S. A. Volume-of-Fluid Simulations in Microfluidic T-Junction Devices: Influence of Viscosity Ratio on Droplet Size. *Phys. Fluids* **2017**, *29* (3), 032007.
(65) Wehking, J. D.; Gabany, M.; Chew, L.; Kumar, R. Effects of Viscosity, Interfacial Tension, and Flow Geometry on Droplet Formation in a Microfluidic T-Junction. *Microfluid. Nanofluid.* **2014**, *16*, 441−453.
(66) Yoon, D.; Tanaka, D.; Sekiguchi, T.; Shoji, S. Structural Formation of Oil-in-Water (O/W) and Water-in-Oil-in-Water (W/O/W) Droplets in PDMS Device Using Protrusion Channel without Hydrophilic Surface Treatment. *Micromachines* **2018**, *9*, 468.
(67) Piccin, E.; Ferraro, D.; Sartori, P.; Chiarello, E.; Pierno, M.; Mistura, G. Generation of Water-in-Oil and Oil-in-Water Microdroplets in Polyester-Toner Microfluidic Devices. *Sens. Actuators, B* **2014**, *196*, 525−531.
(68) Amsden, B. Curable, Biodegradable Elastomers: Emerging Biomaterials for Drug Delivery and Tissue Engineering. *Soft Matter* **2007**, 1335−1348.
(69) Pitt, C. G.; Hendren, R. W.; Schindler, A.; Woodward, S. C. The Enzymatic Surface Erosion of Aliphatic Polyesters. *J. Controlled Release* **1984**, *1*, 3−14.

https://dx.doi.org/10.1021/acs.macromol.0c01300
Macromolecules 2020, 53, 7767−7773